All-solid-state microscope-based system for picosecond time-resolved photoluminescence measurements on II-VI semiconductors

G. S. Buller, J. S. Massa, and A. C. Walker
Department of Physics, Heriot–Watt University, Riccarton, Edinburgh EH14 4AS, Scotland, United Kingdom

(Received 2 December 1991; accepted for publication 13 January 1992)

A novel, entirely solid-state, instrument has been developed for the study of time-resolved photoluminescence in a wide variety of bulk semiconductors, low-dimensional structures, and other materials. This system uses a frequency-doubled GaAlAs diode laser (pulse width 30 ps) as the 415-nm pump source and a silicon single-photon avalanche diode for detection of photoluminescence. The time-correlated single photon counting technique allows measurement of photoluminescence decays in the temporal region of 10 ps to >500 ns with high statistical accuracy. In addition, the combination of a microscope with a small-area detector provides a spatial resolution of <5 μm. This system is currently being used for the measurement of picosecond time-resolved photoluminescence from II-VI semiconductors.

I. INTRODUCTION

The expanding importance of II-VI semiconductors, for example in the fabrication of blue light emitting diodes (LEDs) or laser diodes[1] or for optical switches,[2] has led to increased interest in carrier lifetime studies of these materials. In this paper we describe an all solid-state instrument which is capable of routine time-resolved photoluminescence (TRPL) measurements in the picosecond domain. This instrument has a spatial resolution of only ~ 5 μm, making it suitable for material inhomogeneity studies and the local characterization of different areas within various device structures. It has developed out of earlier work by Louis *et al.*,[3] who constructed a microscope-based system utilizing time-correlated single photon counting (TCSPC), high-repetition rate (50 MHz) picosecond GaAlAs diode laser excitation and silicon single photon avalanche diode (SPAD) detectors. The primary purpose of that system was TRPL measurements on short lifetime GaAs-based devices, particularly solar cells. The instrument described in this paper differs from the previous work in the following ways: (a) a frequency-doubled GaAlAs source is used to permit the examination of band-to-band recombination in wider-gap semiconductors (in particular II-VI materials), (b) a redesigned optical routing module (ORM) allows the efficient detection of PL emission over a wide spectral region (415–900 nm), offering more opportunity to study wavelength-dependent decays, and (c) a variable repetition rate (0–10 MHz) excitation permits a wider temporal dynamic range than previously, allowing the study of longer lifetime material (i.e., >5 ns).

II. INSTRUMENT DESCRIPTION

The system is based on an Edinburgh Instruments photoluminescence lifetime microscope spectrometer (PLμS-2). The 415-nm wavelength source is a variable repetition rate (0–10 MHz) picosecond pulsed GaAlAs diode laser with integral frequency-doubling element. These lasers are sold commercially (Hamamatsu LDH041), and are based on the geometry described by Ohya *et al.*[4] The temporal pulse width is 30 ps (full width at half maximum, FWHM), with a spectral width of 4 nm (FWHM) and, the peak power is ~ 0.3 mW. The detector is a silicon SPAD,[5] with an active area ~ 5 μm in diameter, used in conjunction with an active quenching circuit. It is capable of a timing resolution of 20 ps.[6]

The optical system is constructed around a standard infinite-conjugate microscope (Olympus BH-2). An ORM is inserted into the microscope column in order to permit the following functions: (1) relaying the laser excitation signal to the sample with minimal attenuation, (2) direction of the collected photoluminescence to the SPAD detector, (3) splitting a small part ($\sim 10\%$) of the excitation signal in order to trigger the timing electronics via the secondary avalanche diode, and (4) passing a broadband source to illuminate the sample surface for an imaging charge coupled device (CCD) camera.

The ORM, shown schematically in Fig. 1, consists of a crossed pair of polarizing beamsplitter (PBS) cubes. The upper cube (PBS1) directs the laser excitation signal towards the sample. The operating wavelength of this PBS is centered at approximately the excitation wavelength (415 nm). Hence if *s*-polarized laser light is incident on the cube, then it will be reflected losslessly downwards onto PBS2. Assuming the excitation laser signal is not perfectly *s* polarized, a small component of the beam will be transmitted through the cube to the secondary avalanche photodiode (Optoelectronics Inc. PAD 230) which can act as an optical trigger for the TCSPC timing electronics. This avalanche photodiode is located by the nuclear instrumentation modules (NIM) unit and is connected to the ORM by a multimode optical fiber. The fraction of excitation light routed to this avalanche photodiode can, of course, be altered by the addition of a half-wave plate between the laser and the ORM. PBS2 is broadband coated and has a usable range (50% transmission points) from 400 to ~ 900 nm (Newport PB3). The excitation signal, which is *p* polarized with respect to PBS2, is passed losslessly to the sample via a large numerical aperture (NA >0.65) microscope objective. The isotropically emitted photolumines-

 0034-6748/92/052994-05$02.00

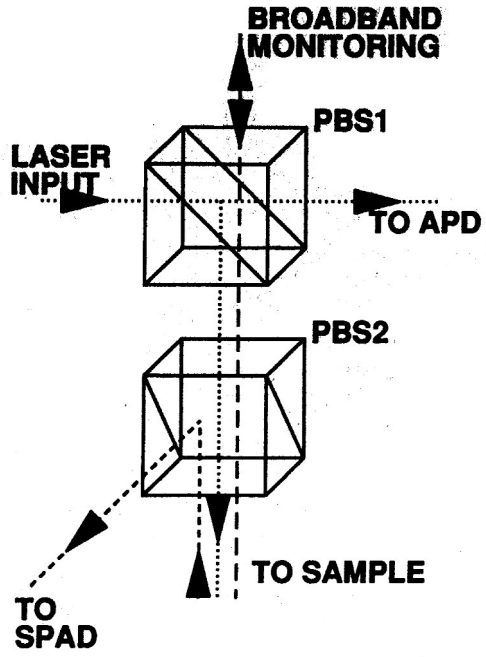

FIG. 1. The optical routing module. (PBS) polarizing beamsplitter, (SPAD) single-photon avalanche diode detector, (APD) secondary avalanche diode.

cence signal is collected and collimated using the full numerical aperture of the objective, and then passed to PBS2, where the s component of the unpolarized signal is reflected towards the SPAD. A high numerical aperture lens is finally used to image the PL signal onto the SPAD.

The spatial resolution of the system depends on the diameter of the active area of the SPAD and the magnification of the detection system—given by the ratio of the focal lengths of the objective and the lens at the SPAD. In this case, an image magnification of 1.5 and a SPAD diameter of 5 μm give a spatial resolution of ~ 3 μm.

The use of a broadband polarizer in PBS2 permits PL signals to be detected right across the range of 415 nm (close to the excitation wavelength) to 900 nm (the upper limit of the PBS). Wavelength discrimination of the detected signal is provided by interchangeable multiple-cavity Fabry–Perot interference filters with a typical bandpass of 5–10 nm (FWHM). Although the specularly reflected laser excitation signal is not of the correct polarization to be reflected at PBS2, a significant proportion ($\sim 1\%$) of this signal does reach the SPAD, due to the limited discrimination of the polarizing beamsplitter, and usefully permits a full instrumental response to be easily measured. This backreflection of excitation signal from the sample is suppressed during the measurement of TRPL decays by the use of a combination of the Fabry–Perot filters and additional edge filters at the SPAD.

The broadband source, used to provide general illumination of the sample for inspection and alignment purposes, is a quartz-halogen lamp which is directed down the microscope column from above. This nonpolarized white light is attenuated at each PBS, but sufficient light is reflected by the sample for the CCD camera (Cohu 4712-2000) to supply a magnified image ($\times 200$) of the surface in the vicinity of the excited area. This facility is particularly useful when examining luminescence from structured materials (e.g., electronic devices, optical waveguides) or in the region of surface defects on wafers.

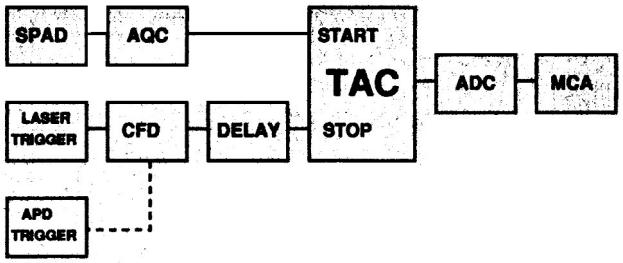

FIG. 2. Schematic of the time-correlated single photon counting set-up used. (AQC) active quenching circuit, (CFD) constant fraction discriminator, (TAC) time-to-amplitude converter, (ADC) analog-to-digital converter, (MCA) multichannel analyzer.

A schematic of the time-correlated single photon counting (TCSPC) setup is shown in Fig. 2. The timing electronics are composed of standard NIM. The TCSPC technique requires that the data collection rate has to be $< 1\%$ of the excitation rate in order that the measured decay is a valid approximation to the PL photon emission probability distribution. The time-to-amplitude converter (TAC) is operated in the reverse mode,[7] whereby the detection of a photoluminescence photon starts the timer and the delayed trigger signal, deriving from the excitation pulse, stops it. This minimizes the dead time of the TAC by operating it only when an actual PL event is detected. The maximum data collection rate is a few 10's kHz, which ultimately is limited by the finite dead time of the analog-to-digital converter (ADC).

The TAC stop pulse is usually taken from the laser driver electronics, with the trigger pulse output being shaped by a constant fraction discriminator (CFD). Although long-term drift (over many minutes) can result in changes in the time interval between the laser pulse and the electronic trigger output, such drift is substantially reduced after several hours of continuous laser operation. With an efficient light collection and detection system, high data acquisition rates can be achieved (> 10 kHz in many cases) and, thus typical data collection times are reduced to only a few minutes (e.g., assuming a 5-ns decay, a TAC conversion gain of 5 ps per channel and a peak of 10^4 counts). Over such time periods drift is < 5 ps and after including the effects of jitter in the timing electronics (TAC, delays and CFDs) and the finite laser pulse width, the use of the laser driver trigger yields an overall instrumental response (FWHM) of typically ~ 65 ps.

An alternative method of generating the (delayed) TAC stop pulse is to use direct detection of the excitation pulse by redirecting a part of the input beam to a secondary avalanche photodiode (see Fig. 1). It was found that, when using the relatively weak 415-nm source and high efficiency illumination of the sample, there was insufficient power available to trigger this avalanche diode reliably. Nonetheless, the optical trigger method has been successfully used

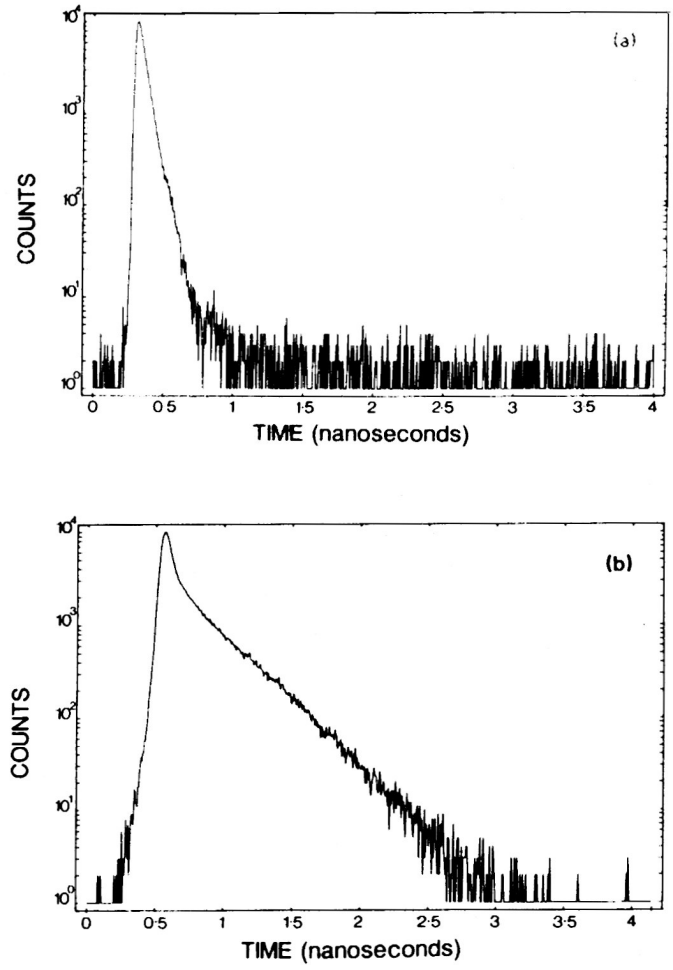

FIG. 3. Instrumental responses, shown on semilogarithmic plots, for (a) the frequency-doubled laser diode source emitting at 415 nm, (b) the GaAs/AlGaAs laser diode source emitting at 780 nm.

in conjunction with a 780-nm picosecond GaAlAs source (Hamamatsu LDH078), where there was an advantage in both the peak power available (>10 mW) and a higher efficiency for the photodiode. This method eliminated any form of long-term drift in the instrumental response although it did appear to add its own contribution to the timing jitter. Thus, for the 780-nm source with typical data acquisition times of several minutes, the instrumental half width was 75 ps when using the laser driver trigger and 100 ps when using the optical trigger. For low efficiency samples which require long data acquisition times (>30 min), there may be a need for optical triggering of the 415-nm source. This could be achieved by using either a more sensitive avalanche diode (e.g., a second SPAD), or a more powerful frequency-doubled source.

III. INSTRUMENTAL PERFORMANCE

A typical instrumental response for the system is shown in Fig. 3. Here, the 415-nm excitation signal is compared with a signal of similar FWHM duration (~ 40 ps) from a 780-nm laser diode (Hamamatsu LDH 078). The full instrumental response (FWHM) is 65 ps for the frequency-doubled laser and 70 ps for the 780-nm diode laser.

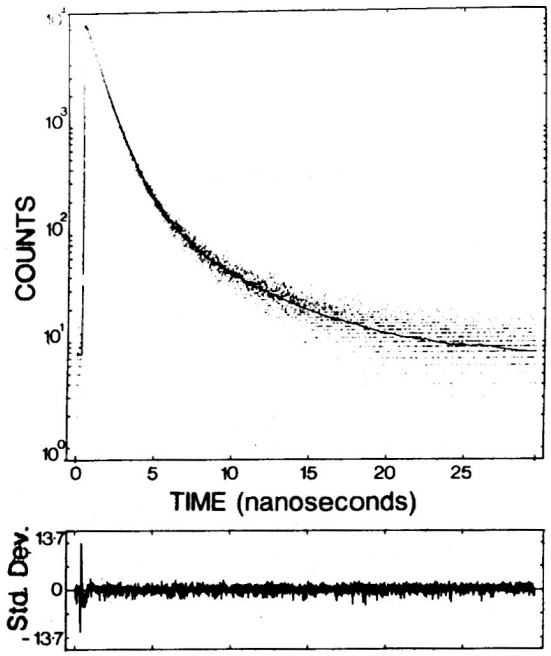

FIG. 4. The time-resolved photoluminescence decay of CVD-grown ZnSe. The raw data are shown on the semi-logarithmic plot, along with the corresponding instrumental response. The data have been fitted to a three-exponential model (solid line) with decay constants (and respective relative amplitudes) of 667 ps (42%), 1.34 ns (43%), and 5.21 ns (15%). The residual distribution is also shown.

However there are substantial differences in the tails of each decay. The full width at 10% of maximum for the 415-nm signal is 160 ps, and 390 ps for the 780-nm signal; while for the 1%-maximum they are 300 ps and 1.2 ns, respectively. The sharper 415-nm instrumental response can be explained by both the nature of the input laser and by its detection. First of all, the frequency doubled pulse tends to be narrower than the fundamental due to the square-law power relation for second-harmonic generation.[4] This has the effect of also reducing the secondary relaxation oscillations which are the inevitable consequence of the gain switching of picosecond semiconductor laser diodes. Second, the significantly higher optical absorption within the silicon SPAD at 415 nm compared with 780 nm means that a higher proportion of carriers will be generated within the avalanche region of the detector.[5] At longer wavelengths free carriers are generated deeper within the structure and diffuse into the avalanche region on a slower timescale (i.e., >100 ps), resulting in an extensive tail on the time response.

IV. TIME-RESOLVED PHOTOLUMINESCENCE OF II-VI SEMICONDUCTORS

An example of a typical photoluminescence decay curve, taken from a bulk chemical vapor deposited (CVD)-grown ZnSe sample, is shown in Fig. 4. This example illustrates the high signal-to-noise ratio that can be achieved by the system—$>1000{:}1$ at the start of the decay. It also shows the high temporal dynamic range of the instrument: both the sub-100-ps instrumental and the >5-ns

tail of the decay both clearly visible. The high signal-to-noise levels obtained by the instrument are achieved despite the low carrier densities excited using the diode laser. The main reasons for the weak excitation are the low peak power of the laser diode ($\sim$0.3 mW) and its highly astigmatic output, which leads to an elliptical illumination area at the sample plane with a size in excess of 5 μm$\times$20 μm. With a peak optical power of 0.1 mW at the sample, and an absorption of $\sim 10^5$ cm^{-1} (Ref. 8) at 415 nm, this corresponds to a peak carrier density of only $\sim 5 \times 10^{14}$ cm^{-3}. Future (second generation) frequency-doubled diode lasers with improved spatial and power outputs should permit the measurement of density-dependent carrier recombination rates as well as improving the signal-to-noise characteristics and/or data acquisition times. It should also be noted that the system is fully compatible with the use of more conventional picosecond dye-laser excitation; if a higher-power tunable pump is required it can be supplied by a fiber positioned in place of the diode laser.

In addition to the raw decay data, Fig. 4 also shows the associated instrumental response and a fit (solid line) based on a three-exponential model. This corresponds to

$$I_{\mathrm{PL}}(t) = A_0 + A_1 e^{(-t/\tau_1)} + A_2 e^{(-t/\tau_2)} + A_3 e^{(-t/\tau_3)},$$

where $I_{\mathrm{PL}}(t)$ describes the temporal dependence of the photoluminescence emission. The fitting was performed using a nonlinear least-squares analysis in which the recorded decay was taken to be an impulse response (i.e., not distorted by the instrumental response). The time constants found were 667 ps (42%), 1.34 ns (43%), and 5.21 ns (15%), where the percentage in brackets refers to the relative amplitude of each component, given by

$$(\text{relative amplitude})_j = \frac{A_j \tau_j}{\Sigma_{i=1-3} A_i \tau_i} \times 100\%.$$

The quality of the fit can be assessed by the value of the normalized chi-squared value ($\chi^2 = 1.05$, in this case) and the analysis of the residual distribution (also shown in Fig. 4). The data analysis was performed on Edinburgh Instruments PLUS software.

The use of reconvolution analysis (i.e., convoluting a model function with the instrumental response) is a second approach which has the advantage of allowing the measurement of decays which are comparable to, or even considerably shorter than the instrumental half width. In the above ZnSe PL decay, reconvolution analysis was not considered necessary but in other cases with PL decay times of less than 100 ps reconvolution analysis is essential. As an illustration of the use of reconvolution analysis in conjunction with the above detection scheme, Louis *et al.*[9] measured a decay time of 10$\pm$2 ps with an instrumental half width of 70 ps. This same detection scheme still retains the versatility to measure decays as long as >100 ns when using a low-repetition rate source (<1 MHz).

It should be noted that with the broad wavelength range over which TRPL measurements can be made, the wavelength dependence of the detector time response (see above) means that a single instrumental function cannot be relied on for deconvoluting those decays with a large shift

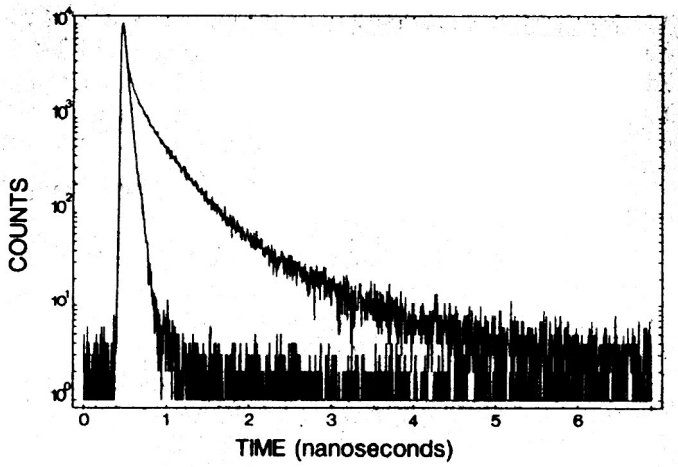

FIG. 5. The time-resolved fluorescence decay of a metal-substituted polydiacetylene at a wavelength of 600 nm. The more rapid decay corresponds to the instrumental response.

from the excitation photon energy. In this case the instrumental response must be derived from a known fast (i.e., less than a few picoseconds) luminescence decay in the appropriate wavelength region.

V. TIME-RESOLVED FLUORESCENCE STUDIES

In addition to TRPL studies of ZnSe, and also CdS, the 415-nm excitation source has permitted time-resolved fluorescence measurements of various organic liquids, including laser dyes, polydiacetylenes, oils, and even single malt Scotch whisky. This significantly extends the range of materials that can be studied beyond those accessible using the alternative 780-nm source—typically used to characterize GaAs/GaAlAs structures.

An example of a rapidly decaying fluorophore, a metal-substituted polydiacetylene, is shown in Fig. 5. Here, the fluorescence decay, detected at 600 nm, is shown along with the instrumental. This example shows the large temporal dynamic range of the instrument, with the initial sub-100-ps decay and the nanosecond tail both resolved. The time constant of the initial part of the decay was found to be 12 ps by reconvolution analysis.

VI. DISCUSSION

We have presented the first picosecond TRPL measurements of ZnSe using an entirely solid-state instrument. This instrument allows *routine* TRPL measurements on a wide variety of semiconductors and other, e.g., organic, materials. Its high spatial resolution also permits studies of both material inhomogeneities and finely structured samples.

Future work on this instrument will take place in four areas: (1) installation of a sample cryostat to permit low-temperature studies of II-VI semiconductors in order to ascertain recombination paths, (2) addition of a high resolution time-compensated monochromator to the instrument to obtain continuous coverage of detected PL emission with 1–50-nm resolution over a wide spectral range,

(3) the possible inclusion of a InGaAsP SPAD to detect PL in the telecommunication wavelength region of 1.3–1.6 μm, (4) the development of a kinetic model for data fitting to directly deduce semiconductor carrier dynamics.

ACKNOWLEDGMENTS

The authors acknowledge the financial support of the United Kingdom Science and Engineering Research Council (SERC) rolling grant No. GR/G11835 and the Royal Society Paul Instrument Fund. JSM is supported by a SERC CASE studentship in collaboration with Edinburgh Instruments Ltd. The SPADs and AQC are used in agreement with Professor Sergio Cova, Milan. The authors wish to thank Dr. Thomas A. Louis, Dr. John R. Gilchrist and Dr. Richard B. Dennis of Edinburgh Instruments Ltd. for regular discussions and Professor S. D. Smith for his encouragement and support.

[1] M. A. Haase, J. Quiu, J. M. DePuydt, and H. Cheng, Appl. Phys. Lett. **59**, 1272 (1991).
[2] J. Oberlé, B. Kippelen, A. Daunois, J. B. Grun, and A. C. Walker, Opt. Commun. (in press, 1992).
[3] T. A. Louis, G. Ripamonti, and A. Lacaita, Rev. Sci. Instrum. **61**, 11 (1990).
[4] J. Ohya, G. Tohmon, K. Yamamoto, T. Taniuchi, and M. Kume, Appl. Phys. Lett. **56**, 2270 (1990).
[5] S. Cova, A. Longoni, and A. Andreoni, Rev. Sci. Instrum. **53**, 408 (1981).
[6] S. Cova, A. Lacaita, M. Ghioni, G. Ripamonti, and T. A. Louis, Rev. Sci. Instrum. **80**, 1104 (1989).
[7] B. T. Turko, J. A. Nairn, and K. Sauer, Rev. Sci. Instrum. **54**, 118 (1983).
[8] S. Adachi and T. Taguchi, Phys. Rev. B **20**, 9569 (1991).
[9] T. A. Louis, G. H. Schatz, P. Klein-Bolting, A. R. Holzwarth, G. Ripamonti, and S. Cova, Rev. Sci. Instrum. **59**, 1148 (1988).